

Structure and Magnetism of Heptanuclear Complexes Formed on Encapsulation of Hexacyanoferrate(II) with the Mn(II) and Ni(II) Complexes of 1,4-Bis(2-pyridylmethyl)-1,4,7-triazacyclononane

Richard J. Parker,[†] Leone Spiccia,^{*†} Boujemaa Moubaraki,[†] Keith S. Murray,[†] David C. R. Hockless,[‡] A. David Rae,[‡] and Anthony C. Willis[‡]

School of Chemistry, PO Box 23, Monash University, Victoria, 3800, Australia, and Research School of Chemistry, Institute of Advanced Studies, Australian National University, Canberra, ACT, 0200, Australia

Received July 5, 2001

The reaction of $[\text{Mn}(\text{dmptacn})\text{OH}_2]^{2+}$ and $[\text{Ni}(\text{dmptacn})\text{OH}_2]^{2+}$ (dmptacn = 1,4-bis(2-pyridylmethyl)-1,4,7-triazacyclononane) with each cyano ligand on ferricyanide results in the assembly of heteropolynuclear cations around the cyanometalate core and reduction of Fe^{III} to Fe^{II} . In $\{[\text{Mn}(\text{dmptacn})\text{CN}]_6\text{Fe}[\text{ClO}_4]_6 \cdot 5\text{H}_2\text{O}$ (**1**) and $\{[\text{Ni}(\text{dmptacn})\text{CN}]_6\text{Fe}[\text{ClO}_4]_6 \cdot 7\text{H}_2\text{O}$ (**2**), ferrocyanide is encapsulated by either six Mn^{II} or Ni^{II} dmptacn moieties. These same products are obtained when ferrocyanide salts are used in the synthesis instead of ferricyanide. A binuclear complex, $\{[\text{Mn}(\text{dmptacn})]_2\text{CN}[\text{ClO}_4]_3$ (**3**), has also been formed from KCN and $[\text{Mn}(\text{dmptacn})\text{OH}_2]^{2+}$. For both Mn^{II} and Ni^{II} , the use of the pentadentate dmptacn ligand facilitates the formation of discrete cations in preference to networks or polymeric structures. **1** crystallizes in the trigonal space group $R\bar{3}$ (No. 148) with $a = 30.073(3)$ Å, $c = 13.303(4)$ Å, and $Z = 3$ and is composed of heptanuclear $\{[\text{Mn}(\text{dmptacn})\text{CN}]_6\text{Fe}\}^{8+}$ cations whose charge is balanced by perchlorate counteranions. Weak H-bonding interactions between neighboring heptanuclear cations and some perchlorate counterions generate an infinite 1D chain of alternating $\{[\text{Mn}(\text{dmptacn})\text{CN}]_6\text{Fe}\}^{8+}$ and ClO_4^- ions running along the c -axis. Complex **3** crystallizes in the orthorhombic space group $Pbcn$ (No. 60) with $a = 16.225(3)$ Å, $b = 16.320(2)$ Å, $c = 18.052(3)$ Å, and $Z = 8$ and is composed of binuclear $\{[\text{Mn}(\text{dmptacn})]_2\text{CN}\}^{3+}$ cations in which the cyano-bridged Mn^{II} centers are in a distorted trigonal prismatic geometry. Variable temperature magnetic susceptibility measurements have revealed the presence of a weak ferromagnetic interaction between the paramagnetic Mn^{II} centers in **1**, mediated either by the $-\text{NC}-\text{Fe}-\text{CN}-$ bridging units or by $\text{Mn}-\text{NH}\cdots\text{ClO}_4^- \cdots \text{NH}-\text{Mn}$ intercluster pathways.

Introduction

The use of hexacyanometalates as templates for the preparation of discrete heteropolynuclear complexes with high-spin ground states^{1–12} as well as heterometallic coordination polymers having one-, two-, or three-dimensional

extended array structures has attracted intense interest over the past decade.^{13–33} Cluster complexes are being investigated for their “single molecule magnet” properties while extended arrays are studied for their 3D long-range order.

* Corresponding author. E-mail: leone.spiccia@sci.monash.edu.au. Fax: +61 3 9905 4597. Phone: +61 3 9905 4526.

[†] Monash University.

[‡] Australian National University.

- (1) Scott, M.; Lee, S.; Holm, R. *Inorg. Chem.* **1994**, *33*, 4651. Scott, M.; Holm, R. *J. Am. Chem. Soc.* **1994**, *116*, 11357.
- (2) Mallah, T.; Auberger, C.; Verdagner, M.; Veillet, P. *Chem. Commun.* **1995**, 61.
- (3) Sculler, A.; Mallah, T.; Verdagner, M.; Nivorozhkin, A.; Tholence, J.; Veillet, P. *New J. Chem.* **1996**, *20*, 1.
- (4) Parker, R. J.; Hockless, D. C. R.; Moubaraki, B.; Murray, K. S.; Spiccia, L. *Chem. Commun.* **1996**, 2789. Parker, R. J.; Spiccia, L.; Batten, S. R.; Cashion, J. D.; Fallon, G. D. *Inorg. Chem.* **2001**, *40*, 4696.

- (5) Van Langenberg, K.; Batten, S. R.; Berry, K. J.; Hockless, D. C. R.; Moubaraki, B.; Murray, K. S. *Inorg. Chem.* **1997**, *36*, 5006.
- (6) Bernhardt, P. V.; Martinez, M. *Inorg. Chem.* **1999**, *38*, 424.
- (7) Arrio, M.-A.; Sculler, A.; Saintetavit, Ph.; Cartier de Moulin, Ch.; Mallah, T.; Verdagner, M. *J. Am. Chem. Soc.* **1999**, *121*, 6414.
- (8) Verdagner, M.; Bleuzen, A.; Marvaraud, V.; Vaissermann, J.; Seuleiman, M.; Desplanches, C.; Sculler, A.; Train, C.; Garde, R.; Gally, G.; Momenech, C.; Rosenman, I.; Veillet, P.; Cartier, C.; Villain, F. *Coord. Chem. Rev.* **1999**, *190–192*, 1023.
- (9) Zhong, Z. J.; Seino H.; Mizobe, Y.; Hidai, M.; Fujishima, A.; Ohkoshi S.; Hashimoto, K. *J. Am. Chem. Soc.* **2000**, *122*, 2952. Zhong, Z. J.; Seino H.; Mizobe, Y.; Hidai, M.; Verdagner, M.; Ohkoshi S.; Hashimoto, K. *Inorg. Chem.* **2000**, *39*, 5095.
- (10) Sra, A. K.; Rombaut, G.; Lahitete, F.; Golhen, S.; Ouahab, L.; Mathoniere, C.; Yakhmi, J. V.; Kahn, O. *New J. Chem.* **2000**, 871.

In one approach to the synthesis of heptanuclear clusters, hexacyanometalates have been reacted with the transition metal complexes of multidentate ligands. Mallah, Verdager, and co-workers^{2,3,7,8} have reported complexes ($[\text{Cr}\{(\text{CN})\text{-ML}\}_6][\text{ClO}_4]_9$) in which six $[\text{M}^{\text{II}}\text{L}]$ units encapsulate one $[\text{Cr}(\text{CN})_6]^{3-}$ ($\text{M} = \text{Ni}$ or Mn ; $\text{L} =$ tetraethylenepentamine or N,N',N'' -tris(2-pyridylmethyl)- N -methyl-ethane)-1,2-diamine). The Ni complex ($S = 15/2$ ground state) shows ferromagnetic coupling ($J_{\text{NiCr}} = 16.8 \text{ cm}^{-1}$) between the Cr^{III} and Ni^{II} centers mediated by the CN bridges. In contrast, the Mn complex ($S = 27/2$ ground state) shows antiferromagnetic coupling ($J_{\text{MnCr}} = -8 \text{ cm}^{-1}$) between Cr^{III} and Mn^{II} . Hashimoto et al.⁹ and Decurtins et al.¹¹ have reported even higher spin ground states for two isostructural cyano-bridged $[\text{Mn}^{\text{II}}_9\text{M}_6^{\text{V}}]$ clusters, $\text{M} = \text{W}$ or Mo , that do not contain chelating coligands. There is some controversy as to the type of coupling since the W cluster displays antiferromagnetism ($S = 39/2$ ground state)⁹ while the Mo cluster shows ferromagnetism ($S = 51/2$ ground state).¹¹

Our interest in the chemistry of pentadentate ligands^{34–40} led us to study the reactions of their metal complexes with hexacyanometalates. We have reported $[\{\text{Mn}^{\text{II}}(\text{dmptacn})\text{CN}\}_6]^{6-}$

$\text{Cr}^{\text{III}}][\text{Cr}^{\text{III}}(\text{CN})_6][\text{ClO}_4]_6 \cdot 6\text{H}_2\text{O}$, a complex which exhibits a short-range ferrimagnetic interaction between the $S = 27/2$ heptanuclear cluster and $[\text{Cr}^{\text{III}}(\text{CN})_6]^{3-}$ anions ($S = 3/2$), mediated through cluster–anion H-bonding (dmptacn = 1,4-bis(2-pyridylmethyl)-1,4,7-triazacyclononane).¹² We report the synthesis, properties, and magnetism of two further examples of heptanuclear complexes, $[\{\text{Mn}(\text{dmptacn})\text{CN}\}_6\text{Fe}][\text{ClO}_4]_8 \cdot 5\text{H}_2\text{O}$ (**1**) and $[\{\text{Ni}(\text{dmptacn})\text{CN}\}_6\text{Fe}][\text{ClO}_4]_8 \cdot 7\text{H}_2\text{O}$ (**2**), and a binuclear complex, $[\{\text{Mn}(\text{dmptacn})\}_2\text{CN}][\text{ClO}_4]_3$ (**3**), whose assembly has been aided by use of the branched N_5 ligand, dmptacn. The crystal structures of **1** and **3** are also reported.

Results and Discussion

Synthesis. Reaction of $[(\text{dmptacn})\text{Mn}(\text{OH}_2)]^{2+}$ or $[(\text{dmptacn})\text{Ni}(\text{OH}_2)]^{2+}$ with hexacyanoferrate(III) in a 6:1 molar ratio yielded two heptanuclear complexes: $[\{\text{Mn}(\text{dmptacn})\text{CN}\}_6\text{Fe}][\text{ClO}_4]_8 \cdot 5\text{H}_2\text{O}$ (**1**) and $[\{\text{Ni}(\text{dmptacn})\text{CN}\}_6\text{Fe}][\text{ClO}_4]_8 \cdot 7\text{H}_2\text{O}$ (**2**). Crystals of **1** suitable for crystallography were obtained on slow evaporation of the resulting pale green solution, while for **2** slow evaporation of the pale pink reaction mixture gave a pale purple powder. The reduction of the cyanometalate core to Fe^{II} is a feature of reactions conducted in water. Heteropolynuclear assemblies with hexacyanoferrate(III) cores can be prepared in dipolar aprotic solvents.⁴² **1** and **2** can be prepared directly from $\text{K}_4[\text{Fe}(\text{CN})_6]$. Encapsulation of the hexacyanoferrate is achieved by capping of each cyanide with one $[\text{M}(\text{dmptacn})]^{2+}$ moiety (see Crystal Structures). The branched dmptacn ligand restricts the formation of coordination polymers since, for metals such as Mn and Ni, only one site is available for bridge formation. Our interest in CN-bridged complexes led us to prepare homobinuclear complexes, which can be byproducts in the synthesis of heterometallic compounds.⁴¹ Here, pale yellow crystals of $[\{\text{Mn}(\text{dmptacn})\}_2\text{CN}][\text{ClO}_4]_3$ (**3**) were formed by reacting $[(\text{dmptacn})\text{Mn}(\text{OH}_2)]^{2+}$ with KCN in methanol

In the IR spectra of **1–3**, N–H stretches at $\sim 3300 \text{ cm}^{-1}$ and pyridyl skeletal vibrations at ~ 1610 , 1570 , and 1470 cm^{-1} confirm the presence of dmptacn. For **3**, a weak ν_{CN} stretch at 2018 cm^{-1} is indicative of end-to-end bridging CN's in binuclear complexes.^{43,44} The ν_{CN} stretch for the heptanuclear complexes (2053 cm^{-1} (**1**) and 2065 cm^{-1} (**2**)) confirms the reduction of the iron core to Fe^{II} , and their position relative to that for $\text{K}_4[\text{Fe}(\text{CN})_6]$ (2042 cm^{-1})

- (11) Larianova, J.; Gross, M.; Pilkington, M.; Audres, H.; Stoeckli-Evans, H.; Güdel, H. U.; Decurtins, S. *Angew. Chem., Int. Ed.* **2000**, *39*, 1605.
- (12) Parker, R. J.; Spiccia, L.; Berry, K. J.; Fallon, G. D.; Moubaraki, B.; Murray, K. S. *Chem. Commun.* **2001**, 333.
- (13) Gadet, V.; Mallah, T.; Castro, I.; Verdager, M. *J. Am. Chem. Soc.* **1992**, *114*, 9213. Mallah, T.; Thiebaut, S.; Verdager, M.; Veillet, P. *Science* **1993**, *262*, 1554.
- (14) Ferlay, S.; Mallah, T.; Ouahés, R.; Veillet, P.; Verdager, M. *Inorg. Chem.* **1999**, *38*, 229.
- (15) Sato, O.; Einaga, Y.; Fujishima, A.; Hashimoto, K. *Inorg. Chem.* **1999**, *38*, 4405.
- (16) Ohba, M.; Maruono, N.; Okawa, H.; Enoki, T.; Latour, J. M. *J. Am. Chem. Soc.* **1994**, *116*, 11566.
- (17) Ohba, M.; Okawa, H.; Ito, T.; Ohto, A. *J. Chem. Soc., Chem. Commun.* **1995**, 1545.
- (18) Ferley, S.; Mallah, T.; Ouahés, R.; Veillet, P.; Verdager, M. *Nature* **1995**, *378*, 701.
- (19) Miyasaka, H.; Matsumoto, N.; Okawa, H.; Re, N.; Gallo, E.; Floriani, C. *Angew. Chem., Int. Ed. Engl.* **1995**, *34*, 1446.
- (20) Miyasaka, H.; Matsumoto, N.; Okawa, H.; Re, N.; Gallo, E.; Floriani, C. *J. Am. Chem. Soc.* **1996**, *118*, 981.
- (21) Ferlay, S.; Mallah, T.; Vaissermann, J.; Bartolome, F.; Veillet, P.; Verdager, M. *Chem. Commun.* **1996**, 2481.
- (22) Salah El Fallah, M.; Rentschler, E.; Caneschi, A.; Sessoli, R.; Gatteschi, D. *Angew. Chem., Int. Ed. Engl.* **1996**, *35*, 1947.
- (23) Re, N.; Gallo, E.; Floriani, C.; Miyasaka, H.; Matsumoto, N. *Inorg. Chem.* **1996**, *35*, 5964 and 6004.
- (24) Michaut, C.; Ouahab, L.; Bergerat, P.; Kahn, O.; Bousseksov, A. *J. Am. Chem. Soc.* **1996**, *118*, 3650.
- (25) Ohba, M.; Fukita, N.; Okawa, H. *J. Chem. Soc., Dalton Trans.* **1997**, 1733.
- (26) Ohba, M.; Okawa, H.; Fukita, N.; Hashimoto, Y. *J. Am. Chem. Soc.* **1997**, *119*, 1011.
- (27) Verdager, M.; Siberchicot, B.; Eyert, V. *Phys. Rev. B* **1997**, *56*, 8959.
- (28) Miyasaka, H.; Okawa, H.; Miyasaka, A.; Enoki, T. *Inorg. Chem.* **1998**, *37*, 4878.
- (29) Colacio, E.; Dominguez-Vera, J. M.; Ghazi, M.; Kivekäs, R.; Lloret, F.; Moreno, J. M. *Chem. Commun.* **1999**, 987.
- (30) Colacio, E.; Dominguez-Vera, J. M.; Ghazi, M.; Kivekäs, R.; Moreno, J. M.; Pajuner, A. *J. Chem. Soc., Dalton Trans.* **2000**, 505.
- (31) Smith, J. A.; Galan-Mascaros, J.-R.; Clerac, R.; Dunbar, K. R. *Chem. Commun.* **2000**, 1077.
- (32) Zhang, S.-W.; Fu, D.-G.; Sun, W.-Y.; Hu, Z.; Yu, K.-B.; Tang, W.-X. *Inorg. Chem.* **2000**, *39*, 1142.
- (33) Zhau, S.; Guo, D.; Zhang, X.; Du, C.; Zhu, Y.; Yan, Y. *Inorg. Chim. Acta* **2000**, *298*, 57.
- (34) McLachlan, G. A.; Fallon, G. D.; Martin, R. L.; Moubaraki, B.; Murray, K. S.; Spiccia, L. *Inorg. Chem.* **1994**, *33*, 4663.
- (35) McLachlan, G. A.; Brudenell, S. J.; Fallon, G. D.; Martin, R. L.; Spiccia, L.; Tiekink, E. R. T. *J. Chem. Soc., Dalton Trans.* **1995**, 439.

- (36) Spiccia, L.; McLachlan, G. A.; Fallon, G. D.; Martin, R. L. *Inorg. Chem.* **1995**, *34*, 254.
- (37) Brudenell, S. J.; Spiccia, L.; Tiekink, E. R. T. *Inorg. Chem.* **1996**, *35*, 1974.
- (38) Fallon, G. D.; McLachlan, G. A.; Moubaraki, B.; Murray, K. S.; O'Brien, L.; Spiccia, L. *J. Chem. Soc., Dalton Trans.* **1997**, 2765.
- (39) Fallon, G. D.; Grannas, M. J.; Nichols, P. J.; Tiekink, E. R. T.; Spiccia, L. *Inorg. Chim. Acta* **1998**, *259*, 192.
- (40) Brudenell, S. J.; Spiccia, L.; Bond, A. M.; Fallon, G. D.; Mahon, P. J.; Hockless, D. C. R.; Tiekink, E. R. T. *Inorg. Chem.* **2000**, *39*, 881.
- (41) Parker, R. J.; Spiccia, L.; Moubaraki, B.; Murray, K. S.; Skelton, B. W.; White, A. H. *Inorg. Chim. Acta* **2000**, *300–302*, 922.
- (42) Parker, R. J. Ph.D. Thesis, Monash University, 1999.
- (43) Bieksza, D. S.; Hendrickson, D. N. *Inorg. Chem.* **1977**, *16*, 924.
- (44) Duggan, D. M.; Jungst, R. G.; Mann, K. R.; Stucky, G. D.; Hendrickson, D. N. *J. Am. Chem. Soc.* **1974**, *96*, 3443.

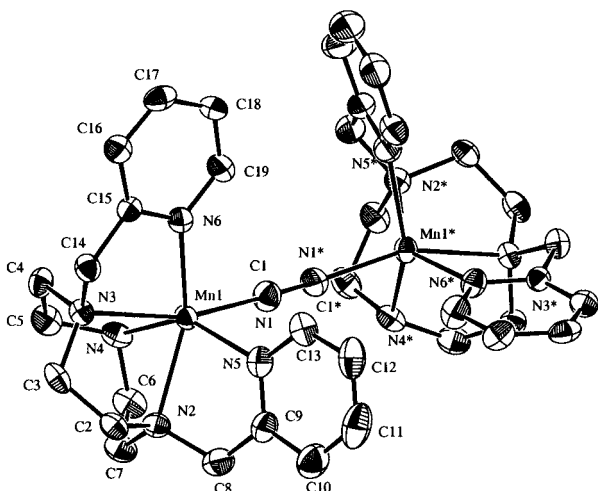


Figure 1. Thermal ellipsoid diagram showing the $\{[Mn(dmptacn)_2CN]\}_2^{3+}$ cation of compound **3**. Asterisks indicate atoms generated by the symmetry operation $(1-x, y, 3/2-z)$. Note that the C and N atoms of the cyanide group are refined as a common site. Ellipsoids show 30% probability levels, and H atoms have been omitted for clarity.

Table 1. Selected Bond Distances (Å) and Angles (deg) of **3** with Esd's in Parentheses

Mn \cdots Mn	5.455(1)	Mn(1)–N(3)	2.314(5)
Mn(1)–C(1)	2.162(6)	Mn(1)–N(4)	2.247(5)
Mn(1)–N(1)	2.162(6)	Mn(1)–N(5)	2.268(6)
Mn(1)–N(2)	2.298(5)	C(1)–N(1) ^a	1.166(8)
Mn–C(1)–N(1) ^a	172.7(6)	N(2)–Mn(1)–N(5)	73.4(2)
N(1)–Mn(1)–N(2)	117.0(2)	N(2)–Mn(1)–N(6)	143.3(2)
N(1)–Mn(1)–N(3)	159.3(2)	N(3)–Mn(1)–N(4)	76.2(2)
N(1)–Mn(1)–N(4)	90.9(2)	N(3)–Mn(1)–N(5)	110.6(2)
N(1)–Mn(1)–N(5)	89.2(2)	N(3)–Mn(1)–N(6)	74.5(2)
N(1)–Mn(1)–N(6)	97.6(2)	N(4)–Mn(1)–N(5)	146.5(2)
N(2)–Mn(1)–N(3)	76.30(17)	N(4)–Mn(1)–N(6)	116.5(2)
N(2)–Mn(1)–N(4)	76.73(18)	N(5)–Mn(1)–N(6)	96.7(2)

^a $1-x, y, 3/2-z$.

indicates CN bridge formation.⁴⁵ The ν_{CN} terminal stretch for $K_3[Fe(CN)_6]$ is found at 2115 cm^{-1} ⁴⁶ while ν_{CN} values for $Fe^{III}-CN-Cu^{II}$ or $Fe^{III}-CN-M^{II}$ assemblies are in the $2140\text{--}2190\text{ cm}^{-1}$ range.^{1,2,46,47} The lack of quadrupole splitting and quite sharp Mössbauer spectra of **1** ($\delta = -0.045\text{ mm s}^{-1}$, $\Delta E = 0.0\text{ mm s}^{-1}$) and **2** ($\delta = 0.020\text{ mm s}^{-1}$, $\Delta E = 0.0\text{ mm s}^{-1}$) also indicate the reduction of the iron core.⁴⁸

Crystal Structures. The X-ray structure of **3** confirms the formation of binuclear cations composed of two $[Mn(dmptacn)]^{2+}$ units connected by one cyano bridge (Figure 1). The dmptacn nitrogens occupy five coordination sites on each Mn^{II} , the sixth site being occupied by the disordered CN ligand. The Mn–C/N distance is $2.162(6)\text{ Å}$ (average Mn–C and Mn–N distances), and the CN bridge is slightly bent, $\{Mn(1)-C/N(1)-N/C(1)^*\}$ (angle = $172.7(6)^\circ$) (Table 1). The distances in other Mn–CN complexes are longer ($2.19(1)\text{--}2.316(4)\text{ Å}$),^{20–23} but these are Jahn–Teller dis-

Table 2. Selected Distances (Å) and Angles (deg) of **1** with Esd's in Parentheses

Fe(1) \cdots Mn(1)	5.056(1)	Mn(1)–N(4)	2.238(8)
Fe(1)–C(1)	1.905(8)	Mn(1)–N(5)	2.238(8)
Mn(1)–N(1)	2.125(7)	Mn1–N(6)	2.184(7)
Mn(1)–N(2)	2.255(1)	C(1)–N(1)	1.166(9)
Mn(1)–N(3)	2.354(7)		
C–Fe–C(cis)	88.3(5), 91.7(3)	N(2)–Mn(1)–N(4)	77.9(3)
C–Fe–C(trans)	180.0	N(2)–Mn(1)–N(5)	75.3(3)
Fe(1)–C(1)–N(1)	178.1(7)	N(2)–Mn(1)–N(6)	150.7(3)
Mn–N(1)–C(1)	154.0(6)	N(3)–Mn(1)–N(4)	77.6(3)
N(1)–Mn(1)–N(2)	103.6(3)	N(3)–Mn(1)–N(5)	89.3(3)
N(1)–Mn(1)–N(3)	170.0(3)	N(3)–Mn(1)–N(6)	75.0(3)
N(1)–Mn(1)–N(4)	92.6(3)	N(4)–Mn(1)–N(5)	152.3(3)
N(1)–Mn(1)–N(5)	100.5(3)	N(4)–Mn(1)–N(6)	102.7(3)
N(1)–Mn(1)–N(6)	105.7(3)	N(5)–Mn(1)–N(6)	97.1(3)
N(2)–Mn(1)–N(3)	76.7(3)		

torted Mn^{III} centers with an axial CN ligand and smaller ionic radius ($Mn^{III}\ 0.79\text{ Å}$ compared to $Mn^{II}\ 0.97\text{ Å}$).⁴⁹ The cyano C–N distance ($1.166(8)\text{ Å}$) is as expected and contributes to a $Mn\cdots Mn$ separation of $5.455(1)\text{ Å}$. Two geometric isomers are possible for 6-coordinate complexes of dmptacn.^{35,40} In one isomer, the CN group is trans to the secondary amine on the tacn ring while in the second isomer it is cis to this amine. As in $[Mn(dmptacn)Cl][ClO_4]$ and related binuclear Mn^{II} complexes,⁴⁰ the second isomer is observed in **3** ($N(4)-Mn-C(1) = 90.9(2)^\circ$).

The trigonal twist angle (ϑ) between the triangular planes defined by the three tacn N's and by the two pyridyl N's and CN donor atom is 24.8° . Thus, the Mn^{II} geometry in **3** is distorted trigonal prismatic, as in $[Mn(dmptacn)Cl][ClO_4]_2$.⁴⁰ The variation in Mn– $N_{dmptacn}$ distances ($2.221\text{--}2.314(5)\text{ Å}$), the puckering of the five-membered chelate rings formed by the pyridyl arms ($Mn(1)-N(2)-C(8)-C(9)$ and $Mn(1)-N(3)-C(14)-C(15)$ torsion angles = 42°), the angles spanned by all chelate rings ($<80^\circ$), and the angles spanned by “trans” donor atoms ($<180^\circ$) correspond to those in $[Mn(dmptacn)Cl][ClO_4]$ and related binuclear Mn^{II} complexes.⁴⁰

Figure 2a shows the asymmetric unit of the heptanuclear cation found in **1**, with the atom-numbering scheme of the unique atoms. The symmetry-expanded projection of the cation (Figure 2b) and space-filling model (Figure 2c) confirm the encapsulation of $[Fe(CN)_6]^{4-}$ by six $[Mn(dmptacn)]^{2+}$ moieties forming the $\{[Mn(dmptacn)CN]_6Fe\}^{8+}$ cations whose charge is balanced by 8 ClO_4^- counteranions. Selected bond lengths and angles are listed in Table 2.

As in other hexacyanoferrate complexes, the Fe^{II} center in **1** is octahedral.^{19,20,22,23,25,26,47,50–56} The C–Fe–C(cis)

(45) Nakamoto, K. *Infrared and Raman Spectra of Inorganic and Coordination Compounds*, 4th ed.; Wiley-Interscience: New York, 1978.

(46) Bertran, J. F.; Pascual, J. B.; Ruiz, E. R. *Spectrochim. Acta* **1990**, *46A*, 685.

(47) Morpurgo, G.; Mosini, V.; Porta, P.; Dessy, G.; Fares V. *J. Chem. Soc., Dalton Trans.* **1981**, 111.

(48) Greenwood, N. N.; Gibb, T. C. *Mössbauer Spectroscopy*; Chapman & Hall, London, 1971.

(49) Cotton, F. A.; Wilkinson, G. *Advanced Inorganic Chemistry*, 5th ed.; John Wiley & Sons: New York, 1988; p 1385.

(50) Lu, Z.; Duan, C.; Tian, Y.; Wu, Z.; You, J. Z. Z.; Mak, T. *Polyhedron* **1997**, *16*, 909.

(51) Chen, Z. N.; Wang, J. L.; Qui, J.; Miao, F. M.; Tang, W. X. *Inorg. Chem.* **1995**, *34*, 2255.

(52) Wu, M. F.; Chen, Z. W.; Qui, J.; Tang, W. X. *Chin. Chem. Lett.* **1994**, *5*, 713.

(53) Miyasaka, H.; Matsumoto, N.; Re, N.; Gallo, E.; Floriani, C. *Inorg. Chem.* **1997**, *36*, 670.

(54) Re, N.; Crescenzi, R.; Floriani, C.; Miyasaka, H.; Matsumoto, N. *Inorg. Chem.* **1998**, *37*, 2717.

(55) Ohba, M.; Usuki, N.; Fukita, N.; Okawa, H. *Inorg. Chem.* **1998**, *37*, 3349.

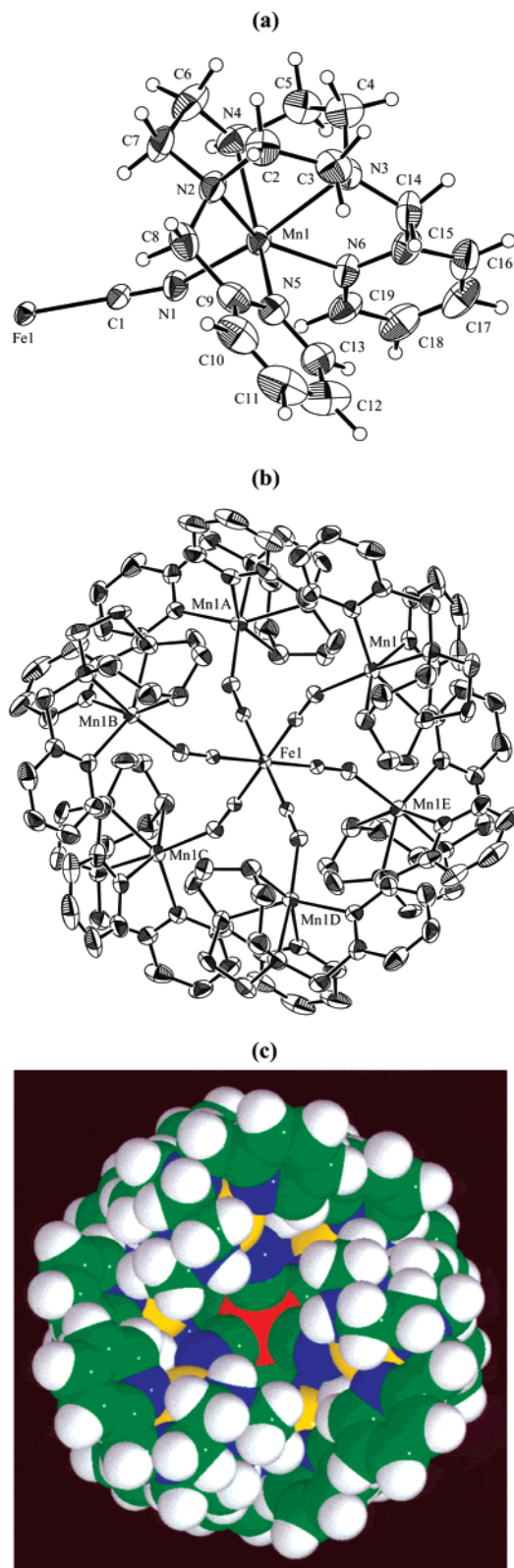


Figure 2. (a) Thermal ellipsoid diagram showing the labeling of atoms in the $[\text{Mn}(\text{dmptacn})\text{CN}]^+$ moiety of compound **1**. (b) Thermal ellipsoid diagram showing the heptanuclear $[\text{Fe}\{\text{Mn}(\text{dmptacn})\text{CN}\}_6]^{8+}$ cation of **1**; H atoms have been omitted for clarity. (c) A space-filling diagram of $[\text{Fe}\{\text{Mn}(\text{dmptacn})\text{CN}\}_6]^{8+}$ showing the toroidal nature of the cation and highlighting one of the open triangular cavities. Ellipsoids in diagrams a and b show 30% probability levels.

angles are either $88.3(4)^\circ$ or $91.7(4)^\circ$, and the C–Fe–C(trans) angles (180.0°) and Fe–C–N angles ($178.1(7)^\circ$)

are linear. In contrast, the Mn–N–C(cyano) angle deviates from linearity ($154.0(6)^\circ$), and to a greater extent than found in **3**. This could be due to steric interactions between dmptacn ligands on adjacent Mn^{II} centers. Although such deviations are found in other Mn–cyanometalate complexes,^{19,20,23,53} these are Jahn–Teller distorted Mn^{III} systems with extended lattices and not discrete molecules such as **1**. The Mn(1)⋯Fe(1) distance in the FeMn_6 cation ($5.056(1) \text{ \AA}$) and the Mn–N(cyano) distances ($2.125(7) \text{ \AA}$) are shorter than for Mn^{III} lattice networks (ranges $5.14\text{--}5.35$ and $2.19\text{--}2.32 \text{ \AA}$, respectively).^{19,20,23,53,57,58}

In **1**, each Mn^{II} center is coordinated to five dmptacn nitrogens and one nitrogen from an iron-bound cyanide located cis to the secondary amine ($\text{N}(1)\text{--Mn--N}(4) = 92.6(3)^\circ$), as for **3** and related systems.⁴⁰ The trigonal twist angle, defined as for **3**, of 44.0° indicates a Mn^{II} geometry that is closer to octahedral than found in **3** and $[\text{Mn}(\text{dmptacn})\text{Cl}][\text{ClO}_4]$, a change that may be reflecting steric and/or electrostatic interactions between adjacent $[\text{Mn}(\text{dmptacn})]^{2+}$ units and ClO_4^- anions. As in **3**, the $[\{\text{Mn}(\text{dmptacn})\text{CN}\}_6\text{Cr}][\text{Cr}(\text{CN})_6][\text{ClO}_4]_6 \cdot 6\text{H}_2\text{O}$ cluster,¹² and related Mn^{II} complexes,⁴⁰ the Mn–N(ligand) distances vary substantially ($2.184\text{--}2.354(7) \text{ \AA}$), the angles spanned by the N's on the tacn rings and the pyridyl pendant arms ($<80^\circ$) are acute, and the trans angle involving the CN ligand is slightly bent ((cyano)N(1)–Mn–N(3) $170.0(3)^\circ$).

Within each cation the six dmptacn secondary amines are organized in two groups, each forming an equilateral triangle on the opposite side of the cation. The two triangles are staggered by 60° (“Star of David” arrangement). The H's on three adjacent secondary amines, also at the corners of an equilateral triangle, participate in weak H-bonding interactions with the O's of the ClO_4^- anion of Cl(5). H-bonding interactions have been found in $[\{\text{Mn}(\text{dmptacn})\text{CN}\}_6\text{Cr}][\text{Cr}(\text{CN})_6](\text{ClO}_4)_6 \cdot 6\text{H}_2\text{O}$, but in this case three triangularly disposed CN's from the $[\text{Cr}(\text{CN})_6]^{3-}$ anions interact with hydrogens on three dmptacn secondary amines of a $[\{\text{Mn}(\text{dmptacn})\text{CN}\}_6\text{Cr}]^{9+}$ cation.¹²

Electronic Spectra. The solution electronic spectrum of **1** exhibits a shoulder at 410 nm ($758 \text{ M}^{-1} \text{ cm}^{-1}$) ascribable to an $\text{Fe}^{\text{II}} \rightarrow \text{Mn}^{\text{II}}$ charge transfer (MMCT) transition. As for $[\text{Ni}(\text{dmptacn})\text{OH}_2][\text{ClO}_4]_2$,³⁴ the solution spectrum of **2** exhibits two of the three d–d bands expected for octahedral Ni^{II} centers, a ${}^3\text{A}_{2g} \rightarrow {}^3\text{T}_{1g}(\text{F})$ transition at 521 nm and a ${}^3\text{A}_{2g} \rightarrow {}^3\text{T}_{2g}$ transition observed as overlapping bands at 814 nm and 883 nm .^{59,60} The solid state spectrum of **2** shows very minor shifts in these d–d bands (see Experimental Section). The ${}^3\text{A}_{2g} \rightarrow {}^3\text{T}_{1g}(\text{P})$ transition normally seen in the $300\text{--}400 \text{ nm}$ region is masked by more intense ligand based and/or $\text{M} \rightarrow \text{L}$ charge transfer transitions.

(56) Fukita, N.; Ohba, M.; Okawa, H.; Matsuda, K.; Iwamura, H. *Inorg. Chem.* **1998**, *37*, 842.

(57) Henkel, H.; Babel, D. *Z. Naturforsch.* **1984**, *39b*, 880.

(58) Mullica, D. F.; Tippin, D. B.; Sappenfield, E. L. *Inorg. Chim. Acta* **1990**, *174*, 129.

(59) Sutton, D. *Electronic Spectra of Transition Metal Complexes*; McGraw-Hill: London, 1968.

(60) Hart, S. M.; Boeyens, J. C.; Hancock, R. D. *Inorg. Chem.* **1983**, *22*, 982.

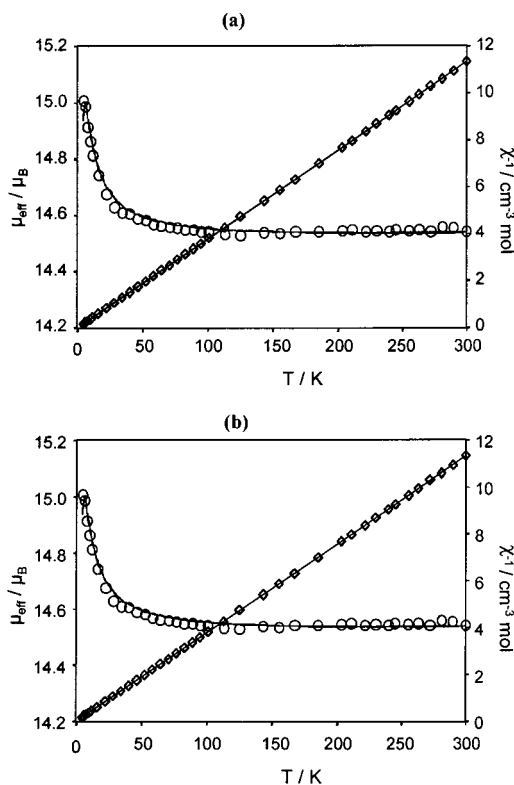


Figure 3. Plots of μ_{eff} (\circ) and χ^{-1} (\diamond) versus temperature (per molecule) for **1** in an applied field of 1 T. The solid line represents best fit to μ_{eff} data using summation of (a) three dimeric $\text{Mn}^{\text{II}}\text{--Mn}^{\text{II}}$ units with $g_{\text{Mn}} = 2.0$, $J = +0.08 \text{ cm}^{-1}$, $\text{TIP} = 120 \times 10^{-6} \text{ cm}^3 \text{ mol}^{-1}$ and (b) two Mn^{II} trimers with $g_{\text{Mn}} = 2.0$, $J = +0.06 \text{ cm}^{-1}$, $\text{TIP} = 180 \times 10^{-6} \text{ cm}^3 \text{ mol}^{-1}/\text{trimer}$.

Magnetic Properties. The magnetic susceptibilities of **1–3** have been measured in the 4.5–300 K temperature range under an applied field of 1 T. Complex **3** displays a room temperature moment ($\mu_{\text{eff}} = 8.01 \mu_{\text{B}}$) that is a little lower than the spin-only value ($8.37 \mu_{\text{B}}$ calculated for two isolated Mn^{II} ($S = 5/2$) assuming $g = 2.00$). As the temperature is decreased, the μ_{eff} value is essentially constant (Curie-like behavior). It remains constant until about 16 K and then decreases to a value of $7.76 \mu_{\text{B}}$ at 4.5 K. The behavior below 16 K suggests that there is a zero-field splitting of the Mn^{II} ($S = 5/2$) states and/or a very weak intramolecular antiferromagnetic interaction via the CN bridge. In accordance with this, the $1/\chi_{\text{M}}$ vs T plot in the 4.5–300 K range obeys the Curie–Weiss law with a small negative Weiss constant ($\theta = -0.31 \text{ K}$).

The room temperature μ_{eff} value of $14.55 \mu_{\text{B}}$ for **1** is in agreement with the spin-only value of $14.49 \mu_{\text{B}}$ expected for a magnetically dilute spin system with one Fe^{II} ($S = 0$) and six Mn^{II} ions ($S = 5/2$) calculated for $g = 2.00$. As the temperature is decreased from 300 to 95 K, the μ_{eff} values remain virtually constant then gradually increase, reaching a maximum value of $15.01 \mu_{\text{B}}$ at 4.5 K (Figure 3). This behavior is suggestive of either weak intercluster ferromagnetic coupling via the H-bonding network or a weak intramolecular ferromagnetic interaction between Mn^{II} ions mediated through the $\text{--NC--Fe}^{\text{II}}\text{--CN--}$ bridge. In accordance with weak ferromagnetism, the $1/\chi_{\text{M}}$ vs T plot, in the range 4.5–95 K, obeys the Curie–Weiss law with a small and positive Weiss constant of $\theta = +0.5 \text{ K}$. In support of

a weak intracluster coupling, Okawa et al.⁵⁶ have reported three different complexes, $[\text{Ni}(\text{L})_2]_3[\text{Fe}(\text{CN})_6][\text{PF}_6]_2$ and $[\text{Ni}(\text{tn})_2]_3[\text{Fe}(\text{CN})_6][\text{ClO}_4]_2$ ($\text{L} = 1,2\text{-diaminoethane (en)}$ or $1,3\text{-diaminopropane (tn)}$), which crystallize in the same crystal system and have extended structures linked by $\text{Fe}^{\text{II}}\text{--CN--Ni}^{\text{II}}$ bridges. These complexes show magnetic behavior similar to that of **1**. The authors proposed a σ -superexchange pathway between the nearest Ni^{II} ions through the empty d_{σ} orbital of the Fe^{II} ion. Thus, an electron spin of the same sign as that of the unpaired electron on the $d_{z^2}(\text{Ni})$ orbital is polarized on the $d_{z^2}(\text{Fe})$ orbital through the filled orbitals of the cyanide bridges. This leads to ferromagnetic coupling between the nearest Ni^{II} ions through the diamagnetic Fe^{II} ion, confirmed in Okawa's complexes⁵⁶ by measurements of the field dependence of magnetization. If the electronic configurations of the ions in **1** are taken into consideration, that is, high-spin Mn^{II} ($t_{2g}^3e_g^2$) and low-spin Fe^{II} (t_{2g}^6), then it is feasible that similar behavior could occur in **1**, as the paramagnetic Mn^{II} ions have an unpaired electron in the d_{z^2} orbital. In addition, the fact that the geometry of the Mn^{II} centers in **1** is distorted octahedral makes a direct comparison between Okawa's example and **1** more pertinent.

The experimental data for **1** was simulated in two ways: first, by a spin Hamiltonian (eq 1) based on the summation of three independent binuclear Mn^{II}_2 units (Figure 3a); $g = 2.0$, $J = +0.08 \text{ cm}^{-1}$, $\text{TIP} = 120 \times 10^{-6} \text{ cm}^3 \text{ mol}^{-1}/\text{dimer}$; second, by a spin Hamiltonian (eq 2) based on the summation of two independent trinuclear Mn^{II}_3 units (Figure 3b); $g = 2.0$, $J = +0.06 \text{ cm}^{-1}$, $\text{TIP} = 180 \times 10^{-6} \text{ cm}^3 \text{ mol}^{-1}/\text{trimer}$. As expected, the J value is very small. Equation 1 (divided

$$\mathcal{H} = -2J(S_1 \cdot S_2 + S_3 \cdot S_4 + S_5 \cdot S_6) + 6g\beta HS \quad (1)$$

$$\mathcal{H} = -2J[(S_1 \cdot S_2 + S_2 \cdot S_3) + (S_4 \cdot S_5 + S_5 \cdot S_6)] + 6g\beta HS \quad (2)$$

by 3) is, of course, applicable to the intracluster possibility in which diamagnetic Fe^{II} centers separate weakly coupled Mn^{II} pairs. While perchlorate bridges, $\text{M--O--Cl(O}_2\text{)--O--M}$, can mediate weak coupling, the ability of H-bonded pathways of the type present in **1** is unknown but expected to be very weak. Our proposal¹² of intercluster coupling between $\text{Cr}^{\text{III}}(\text{CN--Mn}^{\text{II}}\text{L})_6$ clusters might support such a model in **1**, but the nature of the H-bonded pathways is different in each case, and weaker in **1**.

The room temperature μ_{eff} value of $7.26 \mu_{\text{B}}$ for **2** is higher than the spin-only value of $6.93 \mu_{\text{B}}$ expected for a magnetically dilute spin system with one Fe^{II} ($S = 0$) and six Ni^{II} ions ($S = 2/2$), calculated with $g = 2.00$. This is most likely due to second-order spin–orbit coupling effects, a common phenomenon for octahedral Ni^{II} amine complexes. Since, at room temperature, μ_{eff} values for mononuclear Ni^{II} amine complexes are typically in the range $2.80\text{--}3.33 \mu_{\text{B}}$ ($g = 1.98\text{--}2.35$),⁶¹ a μ_{eff} value in the $6.86\text{--}8.15 \mu_{\text{B}}$ range is expected for a system with six Ni^{II} centers. The μ_{eff} of $7.26 \mu_{\text{B}}$ per molecule for **2** is in this range. In a field of 1 T, the

(61) Sacconi, L.; Mani, F.; Bencini, A. In *Comprehensive Coordination Chemistry*, Wilkinson, G., Gillard, R. D., McCleverty, J. A., Eds.; Pergamon: Oxford England, 1987; Vol. 5, p 1.

μ_{eff} value is temperature independent and χ^{-1} is Curie-like. Below 10 K, a slight increase in μ_{eff} could imply very weak ferromagnetic coupling since μ_{eff} normally decreases a little in this region due to zero-field splitting of the Ni^{II} ($S = 1$) centers. Again, this is perhaps more likely to originate from intercluster coupling than to be due to $\text{Ni}^{\text{II}}-\text{NC}-\text{Fe}^{\text{II}}-\text{CN}-\text{Ni}^{\text{II}}$ pathways, proposed by Okawa et al.⁵⁶

Conclusion

Two heterometallic heptanuclear complexes have been assembled around ferrocyanide by capping each cyano group with Ni^{II} and Mn^{II} dmptacn moieties. The structure of the Mn^{II} complex confirmed the formation of quasi-toroidal $[\text{Fe}(\text{CN}-\text{Mn}(\text{dmptacn})_6)]^{8+}$ cations which are stabilized by weak intermolecular interactions between the cations and perchlorate counteranions. A weak ferromagnetic interaction between neighboring Mn^{II} centers in **1** may be mediated through the $-\text{NC}-\text{Fe}-\text{CN}-$ bridges (intracluster) or $\text{NH}\cdots\text{ClO}_4^-\cdots\text{HN}$ H-bonds (intercluster). While the latter is favored by comparison to a $\text{Cr}^{\text{III}}\text{Mn}^{\text{II}}_6$ cluster, which displays ferrimagnetic coupling mediated by H-bonding, the H-bonding pathways are different from those in **1**.

Experimental Section

Physical Measurements. UV–visible–NIR spectra were recorded in the range 200–2500 nm on a Varian Cary 5G spectrophotometer as diffuse reflectance, on solids, or as solutions. Infrared spectra were recorded as KBr pellets on a Perkin-Elmer 1600 series FTIR spectrometer. Electron microprobe measurements were made on a Joel JSM-1 scanning electron microscope through an NEC X-ray detector and pulse processing system connected to a Packard multichannel analyzer. Solid samples were mounted on an aluminum planchet and covered with a thin film of carbon using a Balzer Union CED 010 carbon sputterer. Mössbauer spectra were obtained in the transmission mode using a $^{57}\text{Co}(\text{Rh})$ γ -ray source using literature procedures.⁶² The instrumentation for measuring room temperature magnetic moments was based on a design described elsewhere.⁶³ Variable-temperature magnetic susceptibility measurements on homogeneous powders and/or polycrystalline samples were carried out in the temperature range 2.0–300 K using a Quantum Design MPMS SQUID magnetometer as described previously.⁵ Perchlorate was determined gravimetrically as $\text{Ph}_4\text{AsClO}_4$.

Materials and Reagents. Materials (reagent grade or better) were used as received. 1,4-Bis(2-methylpyridyl)-1,4,7-triazacyclononane (dmptacn),^{3,5} $(\text{Et}_4\text{N})_3\text{Fe}(\text{CN})_6$,⁶⁴ and the Mn^{II} and Ni^{II} dmptacn complexes^{36,40} were prepared by published methods.

CAUTION! Although no problems were encountered in this work, transition metal perchlorates are potentially explosive and should be prepared in small quantities. Care must be taken when handling perchlorate and cyanide salts.

Preparations. $[\{\text{Mn}(\text{dmptacn})(\text{CN})\}_6\text{Fe}][\text{ClO}_4]_8 \cdot 5\text{H}_2\text{O}$ (**1**). **Method A.** An aqueous solution of $\text{K}_3[\text{Fe}(\text{CN})_6]$ (15 mg, 0.047 mmol, in 10 mL of water) was added dropwise to a stirring solution of $[\text{Mn}(\text{dmptacn})(\text{OH}_2)][\text{ClO}_4]_2$ (0.16 g, 0.28 mmol, in 50 mL of water). The green-yellow solution was reduced in volume and

refrigerated at 4 °C overnight to yield green crystals of **1**, which were collected by filtration (yield: 79 mg, 51%).

Method B. An aqueous solution of $\text{K}_4[\text{Fe}(\text{CN})_6]$ (62 mg, 0.19 mmol in 10 mL of water) was added dropwise to a stirring solution of $[\text{Mn}(\text{dmptacn})(\text{OH}_2)][\text{ClO}_4]_2$ (0.58 g, 1.00 mmol in 50 mL of water). The pale green solution was left to slowly evaporate at room temperature. Pale green needles of **1** (0.53 g, 96%) precipitated which were suitable for X-ray crystallography.

Anal. Calcd for $\text{C}_{114}\text{H}_{160}\text{N}_{36}\text{Cl}_8\text{O}_{37}\text{Mn}_6\text{Fe}$: C, 41.5; H, 4.9; N, 15.3. Found: C, 41.5; H, 4.5; N, 15.4. ClO_4^- calcd: 24.2. Found: 24.7. Infrared bands (cm^{-1}): 3420br vs, 3300sh 3070m, 2918s, 2860s, 2052vs, 1607vs, 1571s, 1486vs, 1463vs, 1449vs, 1293s, 1117vs, 1019vs, 942s, 834s, 806s, 779vs, 765vs, 626vs. Electron microprobe: Mn, Fe, Cl present. UV–visible [λ_{max} , nm (ϵ_{max} , $\text{M}^{-1}\text{cm}^{-1}$) in H_2O]: 410 (758). μ_{eff} (295 K): 14.46 μ_{B} per molecule.

$[\{\text{Ni}(\text{dmptacn})\text{CN}\}_6\text{Fe}][\text{ClO}_4]_8 \cdot 7\text{H}_2\text{O}$ (**2**). **Method A.** A solution of $[\text{Et}_4\text{N}]_3[\text{Fe}(\text{CN})_6]$ (70 mg, 0.12 mmol) in CH_3CN (15 mL) was added dropwise to a stirring purple solution of $[\text{Ni}(\text{dmptacn})(\text{OH}_2)][\text{ClO}_4]_2$ (0.41 g, 0.70 mmol) in CH_3CN (20 mL). Following the addition, the brown solution was stirred for an additional 10 min, filtered, and left to evaporate slowly at room temperature. The purple crystalline precipitate of **2** was collected by filtration, washed with water, and then air-dried (yield: 0.37 g, 95%).

Method B. A solution of $\text{K}_4[\text{Fe}(\text{CN})_6]$ (32 mg, 0.086 mmol) in water (20 mL) was added dropwise to a stirring solution of $[\text{Ni}(\text{dmptacn})(\text{OH}_2)][\text{ClO}_4]_2$ (0.26 g, 0.44 mmol) in 30 mL of water. After being stirred for 20 min, the purple solution was filtered and allowed to slowly evaporate, yielding a purple crystalline product, which was collected as in method A. Yield: 0.17 g (69%).

Anal. Calcd for $\text{C}_{114}\text{H}_{164}\text{N}_{36}\text{Cl}_8\text{O}_{39}\text{Ni}_6\text{Fe}$: C, 40.8; H, 4.9; N, 15.0. Found: C, 40.7; H, 4.9; N, 15.1. Infrared bands (cm^{-1}): 3418vs br, 3261s, 2925m, 2870m, 2065vs, 1609vs, 1573m, 1480s, 1448s, 1290m, 1146vs, 1097vs, 1025s, 1002m, 943m, 837m, 767s, 626vs. Electron microprobe: Ni, Fe, Cl present. UV–visible [λ_{max} , nm (ϵ_{max} , $\text{M}^{-1}\text{cm}^{-1}$) in CH_3CN]: 521 (129), 814 (193), 883sh (176). μ_{eff} (293 K): 7.52 μ_{B} per molecule.

$[\{\text{Mn}(\text{dmptacn})\}_2\text{CN}][\text{ClO}_4]_3$ (**3**). A solution of KCN (33 mg, 0.50 mmol) in water (20 mL) was added to an aqueous solution (55 mL) of $[\text{Mn}(\text{dmptacn})(\text{OH}_2)][\text{ClO}_4]_2$ (0.58 g, 1.00 mmol) with stirring. The pale-yellow solution was stirred for 15 min and taken to dryness on a rotary evaporator. Recrystallization of the yellow residue from methanol gave yellow crystals of **3** (yield: 0.16 g, 29%).

Anal. Calcd for $\text{C}_{37}\text{H}_{50}\text{N}_{11}\text{Mn}_2\text{Cl}_3\text{O}_{12}$: C, 42.0; H, 4.8; N, 14.6. Found: C, 41.8 H, 5.0; N, 13.5. Infrared bands (cm^{-1}): 3571vs, 3471vs, 3327vs, 3066m, 2924m, 2194m, 2018m, 1638s, 1609vs, 1572s, 1489vs, 1444vs, 1365s, 1295s, 1097vs, 1017vs, 967m 943vs, 896s, 866vs, 805vs, 777s, 623vs. Electron microprobe: Mn, Cl present. μ_{eff} (290 K): 8.01 μ_{B} per molecule.

X-ray Structure Determination. A green needle of **1**, of ca. $0.28 \times 0.08 \times 0.06$ mm, and a brown prism of **3**, of ca. $0.3 \times 0.3 \times 0.3$ mm, were mounted on glass fibers and used in data collection (Table 3). Measurements were made on a Rigaku AFC6R diffractometer with graphite-monochromated Cu K α radiation (**1**) and a Rigaku AFC6S diffractometer with Mo K α radiation (**3**). The data were collected using the $\omega-2\theta$ scan technique to a maximum 2θ value of 120° for **1** and 45° for **3**. The intensities of three representative reflections were measured after every 150 reflections, and appropriate decay corrections were applied. Empirical absorption corrections based on azimuthal scans of several reflections were applied which resulted in transmission factors in the range 0.56–0.65 for **1** and 0.74–0.80 for **3**. The data were corrected for Lorentz and polarization effects.

(62) Graham, B.; Moubaraki, B.; Murray, K. S.; Spiccia, L.; Cashion, J. D.; Hockless, D. C. R., *J. Chem. Soc., Dalton Trans.* **1997**, 887.

(63) Hill, J. C. *J. Sci. Instrum.* **1968**, *1*, 52.

(64) Mascharak, P. K. *Inorg. Chem.* **1986**, *25*, 247.

Table 3. Crystal Data for **1** and **3**

crystal data	1	3
empirical formula	C ₁₁₄ H ₁₆₀ Cl ₈ FeMn ₆ N ₃₆ O ₃₇	C ₃₇ H ₅₀ Cl ₃ Mn ₂ N ₁₁ O ₁₂
fw, g mol ⁻¹	3295.84	1057.11
space group	R $\bar{3}$ (No. 148)	Pbcn (No. 60)
a, Å	30.073(3)	16.225(3)
b, Å		16.320(2)
c, Å	13.303(4)	18.052(3)
V, Å ³	10419(3)	4780(2)
Z value	3	4
ρ_{calc} , g/cm ³	1.576	1.469
F_{000}	5112	2184
μ , cm ⁻¹	73.0	7.64
temp, °C	-90.0	23.0
λ , Å	1.54178 (Cu K α)	0.71069 (Mo K α)
R ; R_w ^a	0.066; 0.098	0.046; 0.065

$$^a R = \sum(|F_o| - |F_c|) / \sum |F_o|. \quad ^b R_w = [\sum w(|F_o| - |F_c|)^2 / \sum w F_o^2]^{1/2}.$$

The structures were solved by direct methods⁶⁵ and expanded using Fourier techniques.⁶⁶ For **1**, non-H atoms of the cations and water molecules were refined with anisotropic temperature factors and perchlorates with rigid body TLX thermal parametrizations.^{67,68} For **3**, non-H atoms were refined anisotropically. In both cases, H atoms were included at calculated positions and not refined. The final cycle of full-matrix least-squares refinement for **1** was based on 1926 observed reflections ($I > 3\sigma(I)$), 3436 independent reflections and 282 variables while for **3** 1951 observed reflections ($I > 3\sigma(I)$), 3142 independent reflections and 303 variables were used. Neutral atom scattering factors were taken from Cromer and Waber.⁶⁹ Anomalous dispersion effects were included in F_{calc} ;⁷⁰ $\Delta f'$ and $\Delta f''$ values were taken from Creagh and McAuley⁷¹ and mass attenuation coefficients from Creagh and Hubbel.⁷²

The initial structure solution of **1** revealed the cation, anions, and water molecules, but in the ratio of 1:7:6. Chemical evidence, however, indicated an 8+ cation, necessitating a 1:8 cation–anion ratio. We therefore deduced that the anions reside in the water sites $1/6$ of the time, giving rise to the ratio of 1:8:5. The structure of **1** contains ordered cations situated at the origin, site symmetry $\bar{3}$, and its rhombohedral lattice equivalents. Six anions per formula unit are accounted for by an anion 0.787(6):0.213 disordered over two positions, i.e., atoms [Cl(1), O(1)...O(4)] and [Cl(1A), O(1A)...O(4A)]. One anion per formula unit is accounted for by a 1:1 disorder about the $\bar{3}$ site at 0,0, $1/2$. The final anion appears to be randomly oriented and located on just $1/6$ of the sites implied by the general position of O(7). O(7) is from a water molecule that occupies the remaining $5/6$ of these sites. When O(7) is replaced by a ClO₄⁻ ion (denoted Cl(7A) and given a spherically averaged scattering curve), the adjacent ClO₄⁻ ions must change to their minor orientation, denoted by Cl(1A), etc. The anions were constrained in identical tetrahedral geometry with a common refined Cl–O bond length, 1.417(4) Å. Full details are given in the CIF. Constrained refinement utilized the RAELS00 program.⁷³

The cation in **3** possesses crystallographically imposed 2-fold symmetry, and the C and N atoms of the cyanide group are disordered. The disordered atoms appear to coincide, and so N(1) and C(1) have been refined as one site, and the derived Mn–C(1) and Mn–N(1) distances are identical and really express the average value. Whether or not the distances would be equal in an ordered system is unknown. One of the anions is disordered along a 2-fold axis. It has been modeled on two positions, with restraints being imposed upon distances and angles, and the relative populations have been refined. Calculations for this structure were performed using the Xtal crystallographic software package.⁷⁴

Acknowledgment. This work was supported by the Australian Research Council. R.J.P. was the recipient of a Monash Graduate Scholarship. We thank Mr. K. J. Berry for assistance with the fitting of magnetic data and Professor J. D. Cashion for recording Mössbauer spectra.

Supporting Information Available: Two X-ray crystallographic files in CIF format. This material is available free of charge via the Internet at <http://pubs.acs.org>.

IC010711D

- (65) SIR92: Altomare, A.; Cascarano, M.; Giacovazzo, C.; Guagliardi, A. *J. Appl. Crystallogr.* **1993**, *26*, 343.
 (66) DIRDIF94: Beurskens, P. T.; Admiraal, G.; Beurskens, G.; Bosman, W. P.; de Gelder, R.; Israel, R.; Smits, J. M. M. *The DIRDIF-94 program system*; Technical Report of the Crystallography Laboratory; University of Nijmegen: Nijmegen, The Netherlands, 1994.
 (67) Rae, A. D. *Acta Crystallogr.* **1975**, *A31*, 560 and 570.
 (68) Rae, A. D. *Acta Crystallogr.* **1996**, *A52*, C44.
 (69) Cromer, D. T.; Waber, J. T. *International Tables for X-ray Crystallography*; The Kynoch Press: Birmingham, England, 1974; Vol. IV, Table 2.2 A.
 (70) Ibers, J. A.; Hamilton, W. C. *Acta Crystallogr.* **1964**, *17*, 781.
 (71) Creagh, D. C.; McAuley, W. J. *International Tables for Crystallography*; Wilson, A. J. C., Ed.; Kluwer Academic Publ.: Boston, 1992; Vol. C, Table 4.2.6.8, pp 219–222.
 (72) Creagh, D. C.; Hubbell, J. H. *International Tables for Crystallography*; Wilson, A. J. C., Ed.; Kluwer Academic Publ.: Boston, 1992; Vol. C, Table 4.2.4.3, pp 200–206.

- (73) RAELS00, Rae, A. D., Australian National University, Canberra, Australia, 2000.
 (74) Hall, S. R., King, G. S. D., Stewart, J. M., Eds. *Xtal3.4 Reference Manual*; University of Western Australia: Lamb, Perth, Australia, 1995.